AT-90-2-3

#3711

REGIONAL AIRFLOW CHARACTERISTICS IN A MECHANICALLY VENTILATED ROOM UNDER NON-ISOTHERMAL CONDITIONS

J.S. Zhang **L.L. Christianson** **G.L. Riskowski**

ABSTRACT

Experiments were conducted in 38 x 30 x 7 ft rooms and in a 1/12-scale model building to study the effects of thermal buoyancy, diffuser opening, and ventilation rate on room air movement in mechanically ventilated spaces. The decay rate of the diffuser air jet and the average air velocity in the reverse flow, which included the occupied zone, were found to be linearly correlated with the Archimedes number.

INTRODUCTION

Room air movement is an important research issue because it affects the air quality and thermal comfort of the occupants. Local environmental conditions may still be inadequate for occupants due to poor air diffusion within the room, even though the average conditions detected by control sensors are adequate. However, our understanding of room air movement is limited.

Room air movement is a complicated process. In practical cases, it is determined by the building's geometry, diffuser configuration and location, exhaust (return) location, air velocity and direction at the diffuser, ventilation rate, internal obstructions, and thermal buoyancy due to the heat generated by occupants and/or equipment.

Methods commonly used for the study of room air movement are prototype study (full-scale model study), similitude model study (reduced-scale model study), and numerical simulation. Prototype study is important for identifying new phenomena and for evaluating the accuracy of other methods, but it is generally too expensive and inconvenient for studying the effects of a full range of external environments, of internal heat and moisture loads, and of internal obstructions in a full-scale building. Therefore, either the similitude modeling or numerical simulation method is generally used for more detailed study of room air movement.

Previous researchers noted that it is impossible to develop an undistorted similitude model for room air motion when there is internal heat production within the room, because the Reynolds number (ratio of inertial force to viscous force) and Archimedes number (ratio of thermal buoyancy force to viscous force)—both important dimensionless terms in determining room air distribution—lead to contradictory scaling factors (Christianson et al. 1987; Moog 1981). It is expected that flows in different local regions within a room may be dominated by different factors, such as inertial force, thermal buoyancy force, viscous force, or turbulent mixing. Understanding regional flow characteristics in a ventilated building will help to develop methods for correcting distortions in similitude models so the results from a reduced scale model study can be properly extrapolated to the prototype of the model.

In most previous numerical simulation studies of room air flow, a single set of mathematical equations (e.g., the k-ϵ model) is used to describe the entire flow, and studies are limited to highly turbulent flow. However, low turbulent flow is typical in actual residential and office rooms and many specialized applications (e.g., agricultural). One alternative is the approach developed by Lan and Bremhorst (1989) and used by Baker and Kelso (1989), which is a nine-constant k-ϵ model. The additional three constants allow consideration of laminar and low-turbulence flow.

Another alternative is to divide the entire flow field into subfields, each having distinct physical characteristics. Each subfield can be modeled individually, and the combination of all the subfield models then gives a complete picture of the entire flow field. This is called the subfield modeling method, which may result in simpler models for predicting room air diffusion and be able to account for a more realistic ventilation flow situation (Ferziger 1989). Understanding the regional flow characteristics of a ventilated building is essential to the numerical simulation of room airflow with the subfield modeling methods.

The purposes of this study were to (1) investigate the regional flow characteristics within a ventilated space by measurements in actual buildings and in a reduced-scale model room (chamber) with internal heat production and (2) evaluate the effects of thermal buoyancy, diffuser open-

Jianshun Zhang is a Graduate Research Assistant, **Leslie Christianson** is Associate Professor, and **Gerald Riskowski** is an Assistant Professor in Agricultural Engineering at the University of Illinois at Urbana-Champaign.

ing size, and ventilation rate on air velocities in the occupied zone of a typical room.

LITERATURE REVIEW

More and better data are needed on room airflow patterns (Int-Hout 1989). Data are particularly lacking for the low airspeed region of rooms (i.e., outside of the diffuser jet), which usually is the largest portion of the room including the occupied zone. We have not developed the theory needed to extrapolate results from one series of experiments or numerical modeling to another. Furthermore, existing numerical models of room air motion are inadequate for realistic room conditions, partly because we do not have adequate data to assess the model limitations.

Measurement on full- and reduced-scale rooms verifies that:

1. Internal heat production causes a thermal buoyancy effect that significantly affects room airflow patterns. The effect is most important when diffuser air speeds are low (e.g., less than 200 fpm in typical residential rooms) and the internal heat load is high. The Archimedes number can predict when thermal buoyancy is most important ($Ar_c > 75$) and when the incoming air jet is unstable ($30 < Ar_c < 75$) (Randall and Battams 1979).
2. The type and location of air diffusers, the direction of introduced air with respect to the direction of gravity, and the arrangement of internal obstructions strongly affect airflow patterns in the room (ASHRAE 1989; Hellickson and Walker 1983). The influence of room air exhausts is usually negligible, except in cases of low diffuser air speeds and/or improper locations of exhausts relative to the diffusers.
3. Flow fields in rooms with slot diffusers can be practically two-dimensional (Pattie and Milne 1966). Most flow fields are three-dimensional.
4. Airflow in some room conditions is primarily affected by diffuser Reynolds number, while in other cases by Archimedes number, and the scaling methods conflict. In a few cases, room airflows can be modeled by ignoring Reynolds or Archimedes number similarity. More commonly, both are important, but one term dominates (Christianson et al. 1987).
5. There are indications that the room airflow can be divided into flow regions, and that within each flow region, a simpler approach may be used to scale experiments and models (Timmons 1984; Ferziger 1989).

Mathematical modeling efforts of room air movement have progressed as follows:

1. Most efforts are for turbulent, relatively high ventilation rate and airspeed conditions. These conditions do occur in air jet flow regions and in some ventilation cases, but they are not typical of room air conditions in the occupied zones of residences and offices. The commonly used k-ϵ model is a turbulence model developed for highly turbulent conditions (Kusuda 1989).
2. Generalized solution computer models require large computational capabilities (i.e., supercomputers) and even then are limited in their ability to predict airflows in realistic rooms that have internal obstructions and heat sources.
3. There are inadequate measured data to help numerical modelers in development and evaluation of the numerical models (Kusuda 1989; Baker and Kelso 1989).
4. Viewing the room as having several different types of flow, with different equations and constants to describe the flow in these regions, can result in a better, more practical room air model (Ferziger 1989). Alternatively, a k-ϵ model adapted for laminar and low-turbulence flow may improve accuracy in realistic rooms (Baker and Kelso 1989).

PROCEDURES

Field Measurements and Observation

All measurements were made in production swine rooms with approximate dimensions of 38 × 30 × 7 ft. The ventilation rate was approximately 5 to 10 air changes per hour (ach). Air velocities were measured at 17 points in the center section of one room without pigs inside using an omni-directional, temperature-compensated hot wire anemometer; then mean and standard deviation were calculated for each point. Smoke generated by heating mineral oil with a pesticide fogger was used to visualize the flow pattern in the building. In addition, flow patterns were visualized with the smoke method in another swine nursery room and two swine finishing rooms with pigs inside (pigs are the primary internal heat source in swine rooms). All smoke patterns were recorded with a video camera. These field measurements revealed a general airflow pattern typical of mechanically ventilated swine rooms in cold and mild weather.

Reduced-Scale Physical Model Study

The 1/12th-scale model building (43 × 36 × 8 in.) used by Yao et al. (1986) and Christianson et al. (1987) was modified for detailed study of regional flow characteristics (Figure 1). The model building (chamber) had a continuous slot air diffuser and a continuous slot exhaust, both as long as the side walls,[1] so that the flow inside was essentially two-dimensional. Water from the adjustable-setting, constant-temperature water bath was pumped through the uniformly distributed plastic pipes on the floor to simulate an internal heat load. Both the ventilation rate and the diffuser air velocity were controlled by adjusting a valve on the air supply duct. The diffuser air velocity was also adjusted by changing the diffuser opening width[2] while keeping the ventilation rate unchanged.

Mean air velocity and temperature were measured at 60 points (a 5 × 12 grid) in the center section of the model room for seven different testing conditions, using an omni-directional, temperature-compensated hot wire anemometer and a copper-constantan thermocouple, respectively. The flow was maintained at steady state during the measurements.

Smoke generated by electrically heating mineral oil coated on a thin wire was used to visualize the airflow pat-

[1] Both slots have two supports, which block only 6% of the opening area.
[2] Some authors call it opening height, since the diffuser is on a side wall and the width of the opening is the vertical size of the slot.

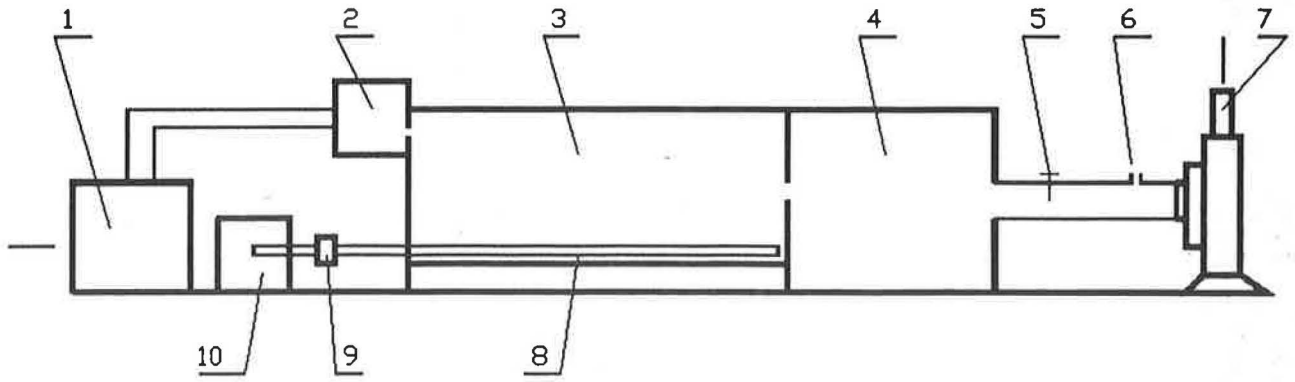

1 : Air conditioner 2 : Inlet duct 3 : 1/12th scale chamber 4 : Outlet plenum 5 : Valve
6 : Hole for measuring air flow rate 7 : Exhaust fan 8 : Water pipe 9 : Water pump
10: Constant temperature water bath

Figure 1 *Experimental set-up for the 1/12th-scale model building (chamber)*

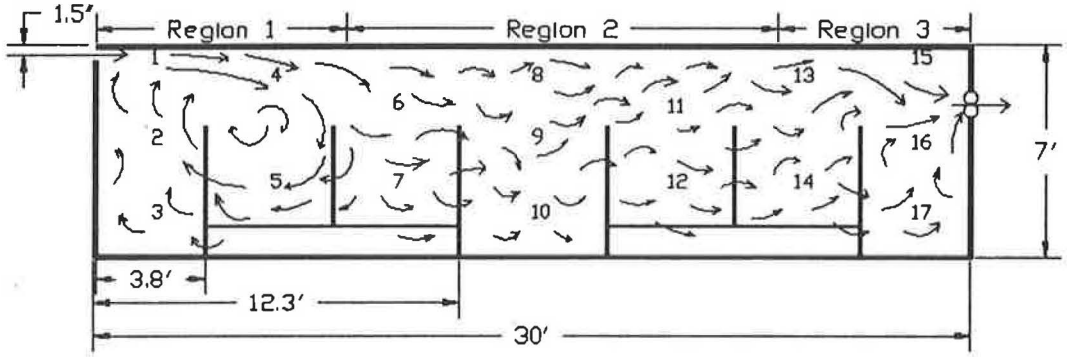

	Region 1					Region 2							Region 3				
P # :	1	2	3	4	5	6	7	8	9	10	11	12	13	14	15	16	17
U/Umax :	1	.33	.48	.49	.31	.16	.06	.05	.02	.06	.15	.06	.29	.05	.98	.43	.18
SD/SDmax:	.65	.46	1	.49	.44	.27	.17	.22	.11	.19	.26	.14	.26	.18	.55	.27	.30

Figure 2 *Air distribution observed in a swine nursery room (38 × 30 × 30 ft). Umax = 400 fpm, SDmax = 278 fpm. The internal obstructions are 4.6 ft high pens with about 70% slot openings on them.*

tern in the model building. A video camera was used to record all the flow patterns for comparisons.

Based on the measurements and flow pattern visualization in the reduced-scale model building, the effects of thermal buoyancy, diffuser opening width, and ventilation rate on the room air distribution were analyzed. The relationships between the decay rate of maximum jet velocity, the velocity in the occupied zone, and the Archimedes number were established.

RESULTS AND DISCUSSION

Field Measurements and Observation

Figure 2 shows the observed airflow pattern with the measured means and standard deviations of the velocities on the center section of a 38 × 30 × 7 ft unoccupied room. Three distinct flow regions were shown: (1) near the diffuser, (2) in the middle, and (3) near the room exhaust on the opposite wall.[3] Air velocities were relatively higher in region 1, which was characterized by a ceiling jet and a large recirculating eddy. In region 2, air traveled with relatively low speed. In region 3, air was accelerated due to the contraction of the exhaust. The higher standard deviations in region 1 might indicate that flow in this region was more turbulent compared to regions 2 and 3, where flow acted more like potential flows. The pen partitions had a significant effect on the airflow distribution and resulted in very low air velocities at points 7, 10, 12, and 14 in regions 2 and 3.

Similar airflow patterns were observed in three other rooms, similar in design, with pigs inside. During the observations, the air was introduced into the building from a continuous slot diffuser on one side wall and exhausted by

[3] These were not intended to be subfields as discussed elsewhere in this paper.

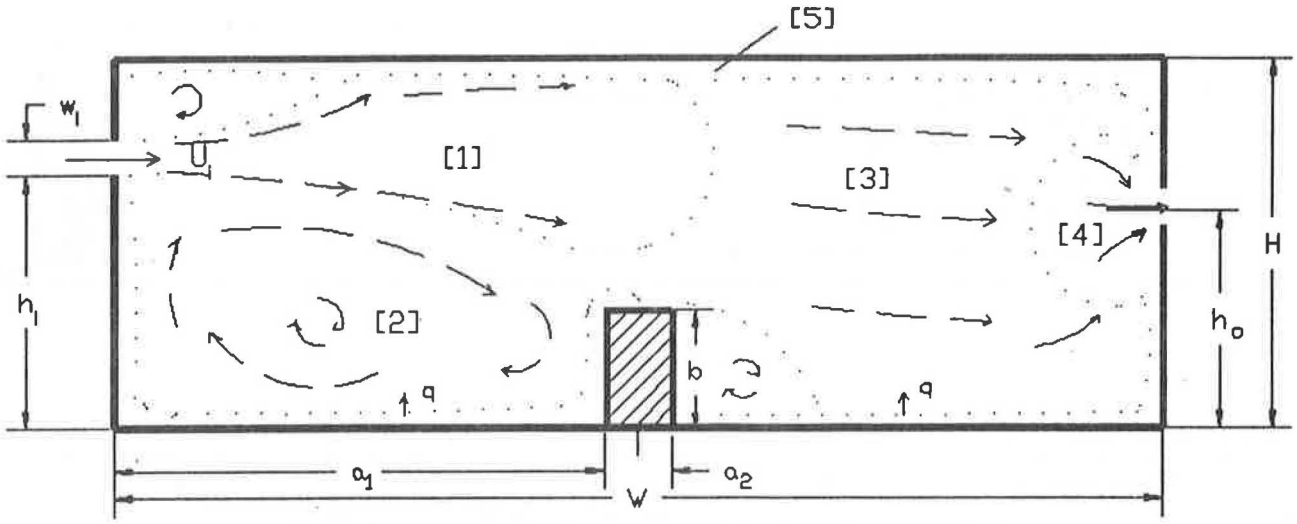

Figure 3 *General air flow pattern in a slot-ventilated building with an obstruction*

TABLE 1
Experimental Conditions[a]

Test #	T_w (°F)	T_i (°F)	U_i (fpm)	w_i (in.)	Q (cfm)	ΔT_a (°F)	Re	Ar (× 10^3)
1	77	76.8	230	3/8	23	32.0	1000	0
2	99	78.9	230	3/8	23	45.7	1000	2.15
3	149	78.6	230	3/8	23	49.6	1000	2.75
4	99	81.5	344	1/4	23	42.2	1000	0.38
5	99	82.4	173	1/2	23	40.1	1000	2.44
6	99	77.0	362	3/8	38	38.1	1120	0.31
7	99	75.2	506	3/8	52	37.6	1550	0.14

[a] All variables are defined in the Nomenclature section.

fan(s) on the other side. It was noted that the thermal buoyancy due to the heat generated by pigs appeared to increase the velocities right above the pigs in the low air velocity region (region 2 in Figure 2). The movement of pigs increased the fluctuation of the air velocities in their immediate vicinity but apparently did not affect the overall airflow pattern within the buildings.

Timmons (1984) reported a secondary recirculating eddy rotating in the opposite direction of the main eddy in measurements of a similar room, but this secondary eddy was not observed in the present study. Perhaps this is because of a much lower diffuser Reynolds number (Re = 4500 to 9000, corresponding to U_i = 550 to 700 fpm and w_i = 1 to 1.5 in.) in the rooms studied, compared to Re = 54,000 (corresponding to U_i = 1122 fpm and w_i = 6 in.) in Timmons' work.

The present study, combined with findings reported by previous researchers, suggests that flow in slot-ventilated buildings generally has the following five types of subfields (Figure 3):

(1) turbulent jet,
(2) recirculation flow,
(3) potential flow,
(4) exhaust (region in immediate vicinity of exhaust), and
(5) boundary layers on solid surfaces of the walls and obstructions.

where subfields (1) and (2) correspond to region 1, subfield (3) to region 2, and subfield (4) to region 3 in Figure 2, respectively. Subfield (5) is added because of the obvious viscous effect in the boundary layers, although the authors were not able to visualize these layers with the smoke method used.

This is a general airflow pattern observed when the ventilation rate[4] is low (approximately 5 to 10 ach). When the ventilation rate increases, the jet will penetrate further toward the opposite wall so that subfield (1) will expand and subfield (3) will contract. For a given configuration and inside arrangement of a building, the whole flow field is dictated principally by the diffuser jet.

The above flow features, therefore, should be included in either a similitude model study or a numerical simulation of room air diffusion. In the similitude study, a scaling factor may be proposed individually for each subfield in which the flow is simpler to describe compared to the whole room, since complete similarity between a reduced-scale model and its prototype is difficult to maintain when both thermal buoyancy and internal obstructions are present in the building. Regarding the numerical simulation, individual models may be developed for each type of subfield, using different simplifying assumptions. The combination of all subfield models then produces a complete picture of the whole flow field. Such a subfield modeling method may result in a simpler mathematical description of ventilation flows, since some effects may be negligible in modeling each subfield.

[4] Ventilation rate is defined as the total airflow through the air diffuser into the room, which could be fresh plus recirculated air.

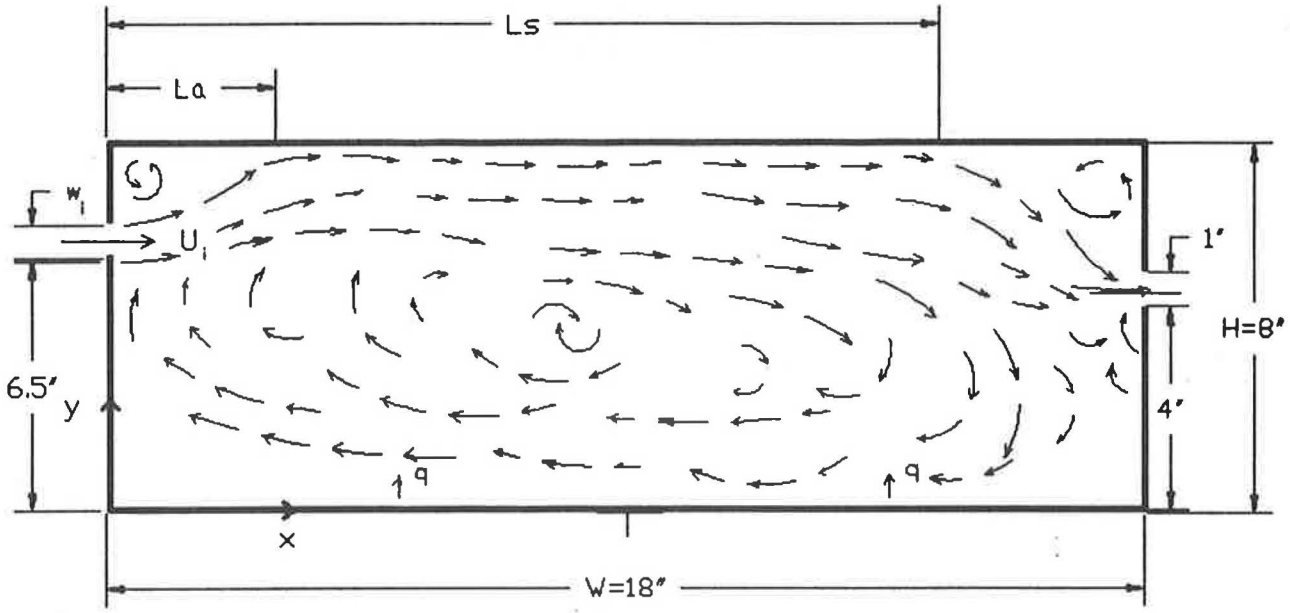

Figure 4 *Flow pattern studied in the 1/12th-scale model building (43 × 18 × 8 in.)*

y/H	Column 1	Column 2	Column 3	Column 4	Column 5
1.00					
0.97	0.14	0.28	0.21	0.13	0.06
0.91	0.17	0.54**	0.51**	0.38	0.22
0.84	0.33	0.42	0.41	0.39**	0.35**
0.78	0.22**	0.21	0.33	0.33	0.31
0.72	0.11	0.09	0.22	0.28	0.29
0.66	0.00*	0.06*	0.16	0.21	0.25
0.59	0.03	0.10	0.15	0.19	0.21
0.53	0.08	0.10	0.11*	0.18	0.19
0.41	0.09	0.12	0.15	0.14*	0.14*
0.28	0.07	0.18	0.19	0.21	0.16
0.16	0.05	0.18	0.24	0.26	0.25
0.03	0.03	0.01	0.21	0.25	0.32
	0	0.06	0.25	0.44	0.61	0.83	1
				x/W			

** Maximum in the column -- Diffuser outlet and return * Minimum in the column

Figure 5a *Velocity distribution (U/U_i) for test 2*
U_i = 230 fpm, w_i = 3/8 in., ΔT_a = 45.7°F

y/H	Column 1	Column 2	Column 3	Column 4	Column 5
1.00					
0.97	0.39	0.44	0.51	0.56	0.51
0.91	0.37	0.37*	0.47	0.52	0.47*
0.84	0.32	0.38	0.45*	0.51*	0.51
0.78	0.21*	0.49	0.50	0.56	0.55
0.72	0.28	0.56	0.61	0.60	0.57
0.66	0.49	0.67	0.68	0.68	0.61
0.59	0.60	0.76	0.73	0.70	0.64
0.53	0.68	0.82	0.79	0.73	0.67
0.41	0.80	0.84	0.81	0.75	0.70
0.28	0.88	0.82	0.80	0.74	0.71**
0.16	0.89	0.88	0.79	0.76**	0.69
0.03	0.90**	1.00**	0.82**	0.73	0.67
	0	0.06	0.25	0.44	0.61	0.83	1
				x/W			

** Maximum in the column -- Diffuser outlet and return * Minimum in the column

Figure 5b *Temperature distribution ($\Delta T/\Delta T_m$) for test 2*
U_i=230 fpm, w_i=3/8 in., ΔT_a=45.7°F, ΔT_m=53.6°F

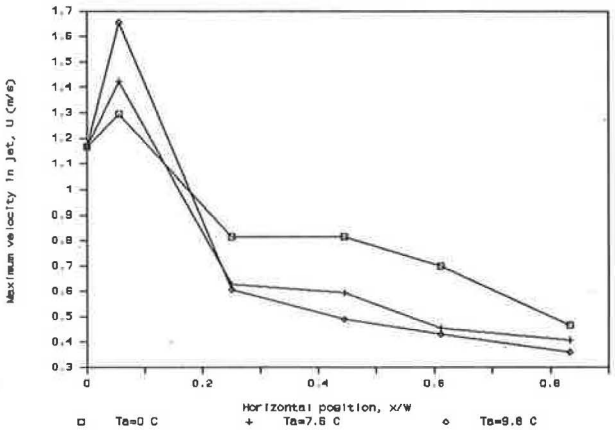

Figure 6 *Effect of thermal buoyancy on jet decay*

Reduced-Scale Physical Model Study

General Analysis of the Airflow Pattern Seven tests were conducted in the 1/12th-scale room (Table 1). The general airflow patterns for these tests were observed with the smoke wire method. They were characterized by a bent free air jet attached to the ceiling, a ceiling jet, and a large recirculating eddy (Figure 4). The air jet was bent due to the Coanda effect.

Figure 5a shows the measured mean velocity distribution for test 2. The decay of maximum jet velocity at measured sections (columns) downstream was clearly identified. The variation of locations at which the maximum velocity occurred indicated that the air jet was bent toward the ceiling due to the Coanda effect, traveled as a ceiling jet for some distance, and then separated from the ceiling. Meanwhile, the jet also expanded due to the entrainment of the ambient room air. The lowest velocity region was at the medium height level (y/H = 0.41 to 0.66), which corresponded to the center of the large recirculating eddy. Air below the level of y/H = 0.41 traveled in the opposite direction of the incoming air jet, forming a reverse flow. Velocities in this reverse flow are of the most concern because this region includes the occupied zone of typical rooms. It can also be seen that the velocity decreased as air traveled toward the diffuser side (from x/W = 0.83 to x/W = 0.06) in the reverse flow. This could be attributed to the retardation of the floor by viscous force and the further mixing with the internal heat load produced by heated water circulating through the pipes at the floor level.

Figure 5b shows the distribution of mean temperature. The low-temperature region was around the diffuser due

TABLE 2
Average Mean Velocity in the Reverse Flow for Different Thermal Buoyancy Effects*

x/W	0.06	0.25	0.44	0.61	0.83	Average
ΔT_a = 32°F	28	39	53	59	47	45
ΔT_a = 45.7°F	12	28	47	55	55	39
ΔT_a = 49.6°F	14	20	41	47	47	33

* Velocities are in fpm and are averages of data at y/H = 0.03, 0.16, and 0.28.

to the injection of cooler air, while the high-temperature region was close to the floor due to the heat generated there. Temperature increased as the air traveled upstream in the reverse flow because of the heat transferred from the floor heat source.

It was intended to reproduce the general airflow pattern observed in the full-scale rooms (Figure 3) in the reduced-scale building. However, to do this, very low diffuser air velocities needed to be maintained, and the room air velocities were even lower. The presently used smoke wire method was not applicable for flow visualization in such a slow ventilation flow, since the thermal buoyancy force exerted on the smoke due to the heat from the wire had a more important effect on the movement of the smoke compared to the room airflow pattern; thus, the smoke pattern could not represent the true flow pattern. In addition, the hot wire anemometer used was unable to sense such a low air velocity with enough certainty because of the effect of the natural convective heat transfer over the heated sensor probe. Therefore, the following discussion is limited to the flow patterns tested (Figure 4), which were characterized by higher than normal ventilation rates.

Effects of Thermal Buoyancy Figure 6 shows the decay of maximum velocity in the jet for three water bath temperatures (T_w) while keeping the diffuser air velocity and opening width the same (tests 1, 2, and 3). When T_w increased and thereby the temperature difference between the inside and outside air (ΔT_a) increased, the maximum velocity (U_m) in the jet decayed faster and to a lower value.

A surprising phenomenon was that the maximum velocities in the jet measured in the section of x/W = 0.06 were higher than the diffuser air velocity. Possibly this is because the section was within the initial region of the jet so that the horizontal velocity was equal to that at the diffuser outlet, while the ambient room air added a vertical velocity component to the jet, resulting in a higher total local maximum velocity in the jet. In other words, the air jet appeared to gain momentum for a short region upon entering the room from the room air flow already established by the previous diffuser jet flow. Another explanation might be the vena contracta, which was approximately 1 inch into the room, and this is plausible since the diffuser had an abrupt geometry change at the outlet. The third possible explanation is that the hot wire anemometer has a temperature-compensation unit (a temperature-sensitive resistor exposed to the flow) above and near the velocity sensor, and some interaction could occur between the thermal wake of the velocity sensor and the temperature-compensation resistor when there is a vertical velocity component, causing an artificially high reading.

Figure 6 also shows that the increasing thermal buoyancy effect (i.e., the increases of ΔT_a) also increased the maximum velocity in the jet (U_m) at this section. All these made the jet flow in a ventilated room much more complicated than an isothermal free jet or wall jet in still ambient fluid. Further measurements are needed to investigate this phenomenon in detail.

The increased internal heat production decreased the average mean air velocity in the reverse flow region (Table 2). This seems to be contradictory to the results from the field measurement, where the thermal buoyancy due to internal heat sources appeared to increase the air velocities right above the sources. This is because the thermal buoyancy had a locally dominating effect in the low-velocity region (region 2 in Figure 2) of the full-scale rooms, while in the reduced-scale model, the thermal buoyancy did not have a locally dominating effect but balanced part of the inertial effect so that a lower air velocity resulted in the reverse flow, compared to the isothermal flow case.

It was also observed with the smoke wire method that the attachment distance (L_a) increased and the separation distance (L_s) decreased due to the increased thermal buoyancy effect, when T_w increased (refer to Figure 4 for the definition of L_a and L_s).

Effect of Diffuser Opening Width with Constant Ventilation Rate The effect of diffuser opening width was determined by varying the diffuser opening size while keeping the ventilation rate and water bath temperature constant (tests 2, 4, and 5). As shown in Figure 7, the thinner jet (i.e., smaller opening width) with higher diffuser air velocity decayed more slowly, resulting in a higher velocity at the section of x/W = 0.833. This means that a thinner jet would penetrate further than a thicker jet in a ventilated room, even though the Reynolds number is the same.

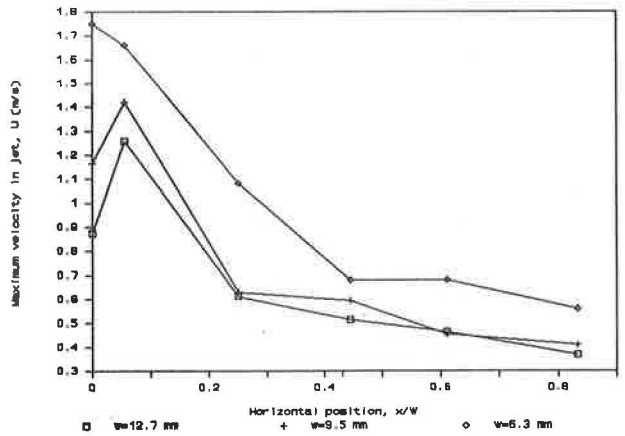

***Figure 7** Effect of inlet opening width on jet decay*

The thinner jet also resulted in a higher average air velocity in the reverse flow (Table 3). This is in agreement with Ogilvie and Barber's (1989) result that floor airspeed increased with the jet momentum number (J), which is pro-

TABLE 3
Average Mean Velocity in the Reverse Flow for Different Diffuser Opening Widths*

x/W	0.06	0.25	0.44	0.61	0.83	Average
w = 1/4 in.	18	28	47	49	45	37
w = 3/8 in.	12	28	47	55	55	39
w = 1/2 in.	20	32	55	51	51	43

* Velocities are in fpm and are averages of data at y/H = 0.03, 0.16, and 0.28.

TABLE 4
Average Mean Velocity in the Reverse Flow for Different Diffuser Air Velocities*

x/W	0.06	0.25	0.44	0.61	0.83	Average	Average/U_i
Q = 23 cfm	12	28	47	55	55	39	34
Q = 38 cfm	22	30	47	61	53	43	23
Q = 53 cfm	22	32	55	69	63	47	18

* Velocities are in fpm.

portional to the product of ventilation rate and inlet air velocity ($J = QU_i/gV$).

It is often desirable to limit the airspeed in the occupied zone while achieving adequate air exchange. The above result suggests that the diffuser air velocity should only be maintained to a level that is just enough to ensure adequate air entrainment and keep the incoming air jet in the desired direction, since excessive diffuser air velocity will result in higher air velocity in the occupied zone (i.e., in the reverse flow).

In addition, the smoke pattern observed indicated that the thinner jet (i.e., less vertical thickness) had a smaller attachment distance. There were two reasons for this. First, the higher diffuser air velocity increased the pressure difference between the upper and lower edges of the jet, which caused the jet to bend toward the ceiling (i.e., the Coanda effect). Second, the higher diffuser air velocity caused the incoming air to be better mixed with the room air before it was exhausted and, as a result, the temperature difference between the inside and outside air was smaller (compare ΔT_a in Table 1 for tests 2, 4, and 5) so there was less thermal buoyancy effect on the jet. The effect of varying diffuser opening width on the separation distance was not clearly shown by the smoke pattern. It would depend upon the relative magnitude of the inertial effect and thermal buoyancy effect. The inertial effect would increase the separation length while the thermal buoyancy effect would decrease it. Additionally, the viscous effect due to the presence of the ceiling would decrease the inertial effect.

Effect of Ventilation Rate The effect of ventilation rate was evaluated by varying the ventilation rate while keeping the diffuser opening size and water bath temperature constant (tests 1, 6, and 7). As the ventilation rate increased, the Reynolds number, based on the diffuser opening width and diffuser air velocity, also increased. As a result, the air velocity in both the jet region and reverse flow region increased (Figure 8 and Table 4), as expected. However, the dimensionless velocity based on the diffuser air velocity (i.e., Average/U_i in Table 4) decreased, which indicated that the dimensionless velocity also depended on the Reynolds number for the flow case studied. This is expected, because it is only for isothermal ventilation flows and where the diffuser Reynolds number is higher than a threshold that the dimensionless velocity is independent

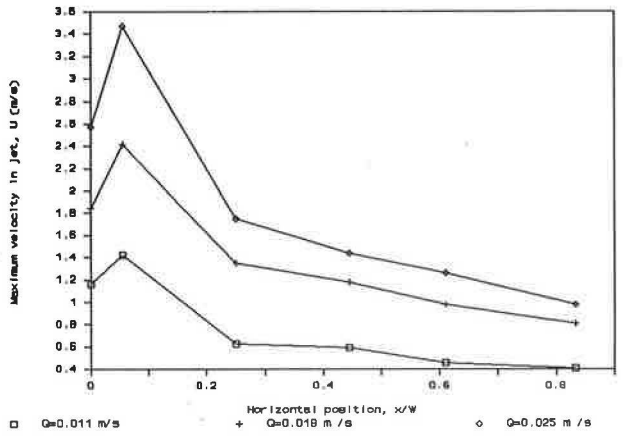

Figure 8 *Effect of ventilation rate on jet decay*

of Reynolds number, as suggested by Pattie and Milne (1966), Timmons (1984), and others.

Additionally, flow visualization with the smoke wire method indicated that the attachment distance decreased with the increase of ventilation rate (essentially the diffuser air velocity), and the separation distance increased. This can be explained by the increased Coanda effect and increased inertial force relative to the thermal buoyancy force because of the increased diffuser air velocity.

Dependence of Jet Decay and Reverse Flow Velocity on Archimedes Number The decay of the maximum velocity in a two-dimensional jet may be described by a function with the following form except for the initial region:

$$\frac{U_m}{U_i} = a\left(\frac{x}{w_i}\right)^{-b} \tag{1}$$

where both a and b are constant. The coefficient b represents the decay rate of the maximum velocity in the jet and is called the decay coefficient of the jet velocity in the present study.

As shown in Table 5 and Figure 9, the decay coefficient increased linearly (in a correlation sense) with the increase of the Archimedes number when the Reynolds number was kept constant. The Archimedes number represents the ratio of thermal buoyancy force to the inertial force. This means that the thermal buoyancy due to the heat genera-

TABLE 5
Regression Constants for the Jet Decay Function*

Test #	1	4	2	5	3
Ar ($\times 10^3$)	isothermal	0.38	2.15	2.44	2.75
Log a	−0.34	−0.51	−0.49	−0.39	−0.57
b	0.31	0.40	0.45	0.44	0.56
R	0.85	0.96	0.98	0.99	0.99

*Re = 1000.

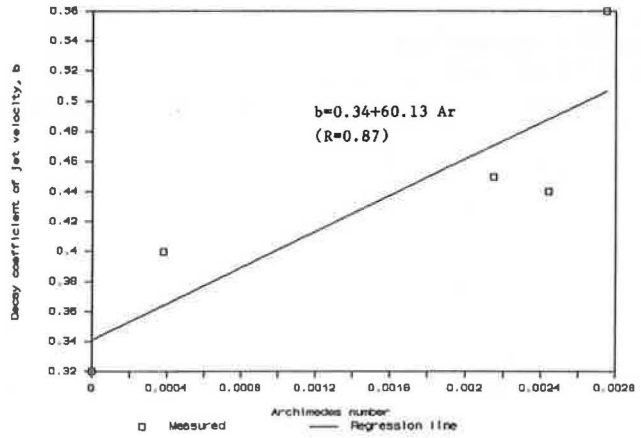

Figure 9 *Dependence of jet decay on Archimedes number*
Re = 1000

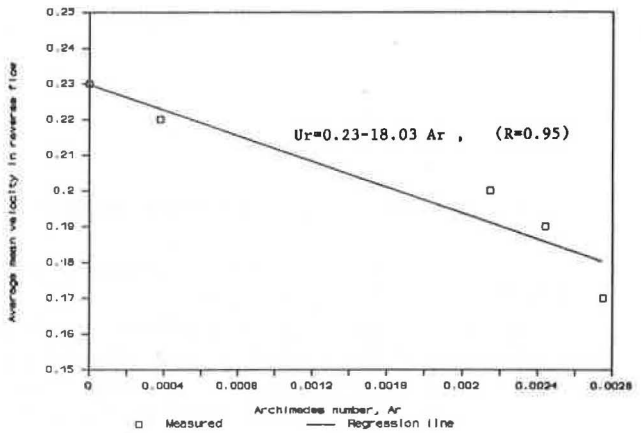

Figure 10 *Dependence of reverse flow velocity on Archimedes number*
Re = 1000

tion from the floor increased the decay rate of the diffuser air jet (i.e., the jet decayed faster).

It is also important to note that the maximum velocity of the isothermal air jet (test1) decayed much more slowly than either an isothermal free jet or wall jet (jets over flat solid surfaces) in a still ambient fluid where the jet is not confined in an enclosure (i.e., by the floor, ceiling, and walls). The decay coefficient for the latter is about 0.5, except in the initial region of the jet (Baturin 1972; Schlichting 1979). The reason is that the ambient room air is also in motion and has a higher vertical velocity component than the jet. This is essentially because of the confinement of the floor, walls, and ceiling. Therefore, when modeling the diffuser air jet in a ventilated room, the effects from the ambient room air have to be included.

Figure 10 shows a linear correlation between the measured average mean velocity in the reverse flow and the Archimedes number for a constant Reynolds number. For a different diffuser Reynolds number, a different linear correlation between the average velocity in the reverse flow and Archimedes number is expected. Both Archimedes number and Reynolds number will be important in determining the air velocity in the occupied zone.

SUMMARY AND CONCLUSIONS

1. The velocity measurements and flow visualization in rooms with internal obstructions and heat sources suggested that the whole flow field may be divided into five types of subfields, and a subfield modeling method may be used for developing mathematical models of room air distribution in ventilated spaces.
2. Experiments in a reduced-scale room were conducted for flow fields characterized by a turbulent horizontal jet directed along the ceiling and a large recirculating eddy. The following results were obtained:
   (a) Increasing thermal buoyancy due to the floor heat source increased the decay rate of the maximum velocity in the diffuser air jet and decreased the average mean velocity in the reverse flow region, which included the occupied zone. It also increased the distance at which the jet attached to the ceiling and decreased the distance at which the jet separated from the ceiling.
   (b) For the same ventilation rate, increasing the diffuser air velocity by reducing the diffuser opening size increased the air velocity in the reverse flow region, and the incoming air was better mixed with the room air before it was exhausted. Therefore, when it is desired to minimize airspeeds in the occupied zone, the diffuser air velocity should be kept just high enough to ensure adequate air mixing and to maintain the air jet traveling in the desired direction.
   (c) Increasing ventilation rates by increasing the diffuser velocity, which means an increase in the diffuser Reynolds number, caused the air velocity in the occupied zone to increase. However, the ratio of the velocity in the occupied zone to the diffuser air velocity decreased. Therefore, air distribution in a ventilated building with internal heat production is generally Reynolds number dependent, except for isothermal and highly turbulent flow.
   (d) For the same Reynolds number, the decay rate of the maximum local velocity in the jet increased linearly with increasing Archimedes number. The ratio of the average mean velocity in the occupied zone to the diffuser air velocity decreased linearly.

NOMENCLATURE

A = area of the diffuser outlet (ft^2)

Ar = Archimedes number, defined as $\frac{\beta g w_i \Delta T_a}{U_i^2}$

Ar_c = corrected Archimedes number, defined as $\frac{0.6A}{D}Ar$

a = constant in the velocity decay function of the air jet

b = decay coefficient of the air jet

D = characteristic dimension of a room, defined as $(2WH)/(W + H)$

g = gravitational acceleration (ft²/min)

J = jet momentum number, defined as $(QU_i)/(gV)$

L_a = attachment length of the air jet (Figure 4), (ft)

L_s = separation length of the air jet (Figure 4), (ft)

Q = ventilation rate (cfm)

q = heat generated by the floor (Btu/ft²)

R = correlation coefficient

Re = diffuser Reynolds number, defined as $(U_i w_i)/(\nu)$

SD = standard deviation of velocities (fpm)

$SDmax$ = maximum standard deviation of velocities at measured points (fpm)

T_i = air temperature at the diffuser outlet (°F)

T_w = water temperature in the water bath (°F)

U = air velocity at the measured points (fpm)

U_i = diffuser air velocity (fpm)

U_m = maximum velocities in the jet at the measured sections (fpm)

$Umax$ = maximum velocities at the measured points (fpm)

Ur = average velocity in the reverse flow region (fpm)

V = room volume (ft³)

w = width of the building (ft)

w_i = width of the inlet opening (ft)

x = horizontal coordinate (ft)

y = vertical coordinate (ft)

Greek Symbols

ΔT = temperature difference between inside and outside air for a measured point (°F)

ΔT_a = average temperature difference between the inside and outside air for a measured point (°F)

ΔTm = maximum temperature difference between the inside and outside air (°F)

β = thermal expansion coefficient $(1/R)$

ν = kinematic viscosity (ft²/min)

REFERENCES

ASHRAE. 1989. *ASHRAE handbook—1989 fundamentals,* chapter 31. Atlanta: American Society of Heating, Refrigerating, and Air-Conditioning Engineers, Inc.

Baker, A.J., and Kelso, R.M. 1989. "Computational fluid dynamics procedures applied to prediction of room air motion." Report CFDL/89-2, Department of Engineering Science and Mechanics, University of Tennessee, Knoxville, TN.

Baturin, V.V. 1972. *Fundamentals of industrial ventilation.* Translated by O.M. Blunn. New York: Pergamon Press.

Christianson, L.L.; Riskowski, G.L.; Zhang, J.S.; and Koca, R. 1987. "Predicting air velocity at the pig level." *Proceedings of International Livestock Environment Symposium.* St. Joseph, MI: American Society of Agricultural Engineers.

Ferziger, J.H. 1989. "Application of zonal modeling to ventilation simulation." In *Building Systems: Room Air and Air Contaminant Distribution* (Ed., L.L. Christianson). Atlanta: American Society of Heating, Refrigerating, and Air-Conditioning Engineers, Inc.

Hellickson, M.A., and Walker, J.N. 1983. *Ventilation of agricultural structures.* An ASAE monograph. St. Joseph, MI: American Society of Agricultural Engineers.

Int-Hout, D., III. 1989. "Physical modeling." In *Building Systems: Room Air and Air Contaminant Distribution* (Ed., L.L. Christianson). Atlanta: American Society of Heating, Refrigerating, and Air-Conditioning Engineers, Inc.

Kusuda, T. 1989. "Mathematical modeling." In *Building Systems: Room Air and Air Contaminant Distribution* (Ed., L.L. Christianson). Atlanta: American Society of Heating, Refrigerating, and Air-Conditioning Engineers, Inc.

Lam, C.K.G., and Bremhorst, K. 1981. "A modified form of the kmodel for predicting wall turbulence." *Transactions of the ASME,* Vol. 103, pp. 456-460.

Miller, P. 1989. "Descriptive methods." In *Building Systems: Room Air and Air Contaminant Distribution* (Ed., L.L. Christianson). Atlanta: American Society of Heating, Refrigerating, and Air-Conditioning Engineers, Inc.

Moog, I.W. 1981. "Room flow tests in a reduced scale." *ASI IRAE Transactions,* Vol. 87, Part 1, pp. 1162-1181.

Ogilvie, J.R., and Barber, E.M. 1989. "Jet momentum number: an index of air velocity at floor level." In *Building Systems: Room Air and Air Contaminant Distribution* (Ed., L.L. Christianson). Atlanta: American Society of Heating, Refrigerating, and Air-Conditioning Engineers, Inc.

Pattie, D.R., and Milne, W.R. 1966. "Ventilation air flow patterns by use of models." *ASAE Transactions,* Vol. 9, No. 5, pp. 646-649.

Randall, J.M., and Battams, V.A. 1979. "Stability criteria for airflow patterns in livestock buildings." *J. Agric. Engrg. Res.,* Vol. 24, No. 4, pp. 361-374.

Schlichting, H. 1979. *Boundary layer theory,* 7th edition. New York: McGraw Hill Book Co.

Timmons, M.B. 1984. "Use of physical models to predict the fluid motion in slot-ventilated livestock structures." *ASAE Transactions,* Vol. 27, No. 2, pp. 502-507.

Yao, W.Z.; Christianson, L.L.; and Muehling, A.J. 1986. "Air movement in neutral pressure swine buildings—similitude theory and test results." ASAE Paper 86-4532.